MINERALOGICAL MAGAZINE

VOLUME 48 NUMBER 346 MARCH 1984

Mafic silicates from the nepheline syenites of the Motzfeldt centre, South Greenland

A. P. JONES*

The University of Chicago, Department of Geophysical Sciences, 5734 South Ellis Avenue, Chicago, Illinois, USA 60637

ABSTRACT. At least five successive intrusions of nepheline-bearing magmas fractionated *in situ* and developed repeatedly overlapping, yet distinct chemical trends in the mafic silicates. Representative electron probe analyses are given for olivine, clinopyroxene, amphibole, biotite, and aenigmatite and their variations discussed. Increasing Na with fractionation produced aegirine-rich clinopyroxene and caused Na/K in amphibole to increase from 2.4 to 7.0. Si^z/Al^z increased in both amphibole and in the less abundant mica. Mn-enrichment is common to all of the mafic silicates, including the olivines and it is suggested that the parent magmas were initially Mn-rich.

Mineralogically the Motzfeldt centre is evolved and similar to the other centres in the Igaliko complex. However, the Motzfeldt centre contains the most fractionated rocks (lujavrites) and is in this respect similar to the peralkaline Ilímaussaq intrusion. The compositional ranges and trends of the mafic silicates in Motzfeldt thus provide links between the uncommon peralkaline plutons and the more abundant and typical nepheline syenites.

THE PROCESSES which lead to the emplacement of large plutonic 'batholiths' of alkaline and peralkaline magma into shallow levels of the crust are poorly understood. Good exposures throughout the Gardar province in southern Greenland (for general description see Upton, 1974; Emeleus and Upton, 1976) give a clear indication of prolonged Proterozoic alkaline magmatism (~ 1350–1150Ma) associated with tectonic rifting, which produced many plutonic centres. The dominant message which comes from the studies of these centres is one of multiple overlapping intrusions. Vertical sections to a height of nearly 2 km are typical, no bases are seen and there are remarkable repetitions in rock types from geographically distant centres. These features, together with their small range in initial $^{87}Sr/^{86}Sr$ ratios (Blaxland *et al.*, 1978) of ~ 0.702–0.710, indicate volumes of magma on a crustal-forming scale and as such are rather similar to the extensive batholiths (tonalitic) of Peru (Pitcher and Bussell, 1977).

Perhaps the most celebrated and unique centre in the Gardar province is the Ilímaussaq intrusion (Ferguson, 1970) whose formation and genetic precursor remains enigmatic. Of all the other centres, the Motzfeldt centre is unique in that it developed a separate late-stage peralkaline magma with a characteristic mineralogy similar to those at Ilimaussaq. The dominant mineral throughout the nepheline syenites is, of course, alkali feldspar, closely followed by nepheline. However, it is the mafic mineralogy which best records crystallization events spanning the entire range from liquidus to late-stage interstitial phases. The mafic silicates tend to amplify parallel fractionation trends which presumably occurred in the bulk magmas of each intrusive unit. Table I presents a schematic representation of the typical order of crystallization in the Motzfeldt nepheline syenites, and although this is a gross simplification, provides a basic framework for the rest of the text.

Geological summary

The Motzfeldt centre is one of four centres of alkaline igneous activity which form the Igaliko complex and has been described by Emeleus and Harry (1970). It is situated near the extreme east of

---

* Present address: Division of Geological and Planetary Sciences, California Institute of Technology, Pasadena, CA 91125, USA.

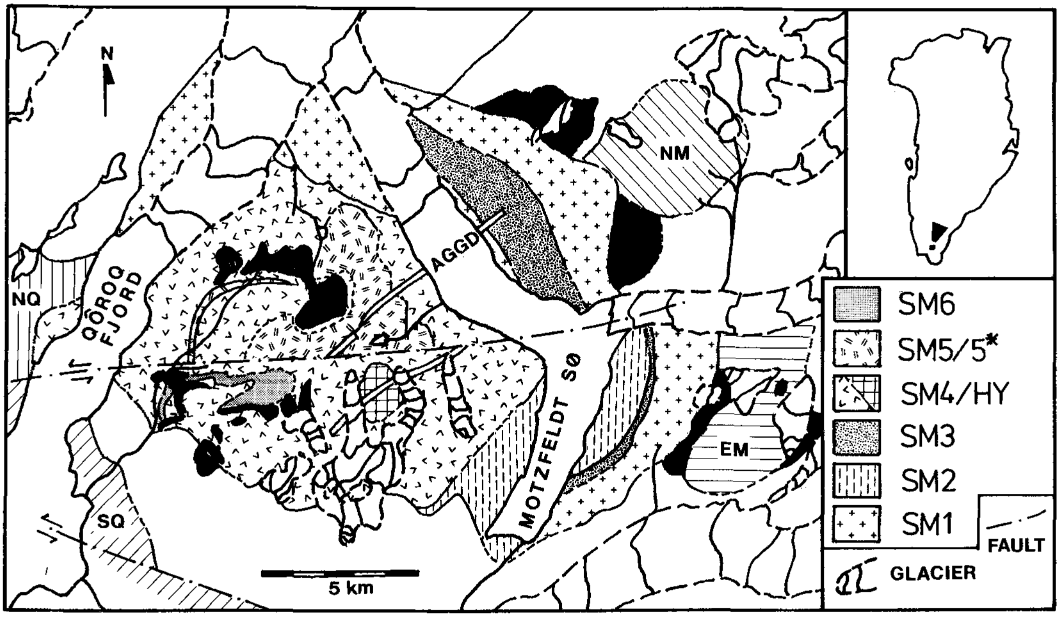

FIG. 1. Schematic map of the Motzfeldt centre with major syenite units prefixed 'SM' and numbered 1-6 in order of emplacement; AGGD is alkali gabbro giant dyke. *Satellitic syenites*: EM = East Motzfeldt; NM = North Motzfeldt (two units). *Ornamentation*: black = supracrustal rocks (Eriksfjord Formation) both outside centre and incorporated as xenolithic rafts. NQ = North Qôroq centre, SQ = South Qôroq centre. Compiled from Jones (1980), Emeleus and Harry (1970), and Stephenson (1972, 1973).

the alkaline Gardar province (Upton, 1974; Emeleus and Upton, 1976) and was emplaced into country rock gneiss. The Motzfeldt centre has a low initial $^{87}Sr/^{86}Sr$ ratio of 0.702 and a Rb-Sr age of 1310 ± 31 Ma (Blaxland *et al.*, 1978). The centre was emplaced by a combination of 5-10 km radius ring fracture and block stoping and covers approximately 350 km^2. It can be considered to consist of essentially six major units (see map, fig. 1) of silica-undersaturated syenites, numbered SM1 to SM6 in order of emplacement and a late alkali gabbro giant dyke (AGGD). Each of the units has undergone varying degrees of fractionation *in situ* and is represented by a variety of rock types, which commonly exhibit cumulus textures similar to the other centres of the Igaliko complex and throughout the Gardar province. Several of the large syenite units (unit SM4 in particular) contain numerous and sometimes very large raft-like xenoliths (up to 3 km long and ~ 100 m thick) of supracrustal lavas and volcaniclastic rocks. The xenoliths are altered and metasomatized to different degrees, and may in part represent a suite of alkaline lavas genetically related to the centre itself (Jones, 1980).

Table I. Schematic crystallisation sequence for the nepheline syenites

Feldspar + Nepheline	
Olivine	
Clinopyroxene	
Amphibole	
Fe-Ti oxides	Aenigmatite
	Mica
→ INCREASING CRYSTALLISATION	Natrolite *etc*.[†]

[†] includes other accessory phases such as sphene, rinkite, rinkolite, låvenite, eudialyte, fluorite, sodalite and cancrinite (all late). Apatite is an early-formed accessory phase (not indicated above).

Smaller 'satellitic' intrusions of syenite (EM and NM in fig. 1), younger plugs of ultrabasic and carbonatitic affinities, and a large number of regionally aligned (ENE) dykes, which all cut the centre, are not considered here.

Brief description of the syenite units. Unit SM1 may have covered an original area of approximately 180 km^2 (Jones, 1980), much of which has been cored out by the younger units. It is typically a coarse-grained syenite (~ 1 cm feldspar) with characteristic anhedral areas of mafic minerals dominated by amphibole. Nepheline varies from 0 to 20% of the mode; quartz is always absent. The bulk composition ranges from trachytic to phonolitic and the most fractionated varieties are peralkaline. *Unit SM2* grades from cumulus textured and porphyritic nepheline syenite to phonolite, with a partial change from stable Fe–Ti oxides to aenigmatite. *Unit SM3* is a partial ring dyke of porphyritic phonolite or nepheline microsyenite, with phenocrysts of alkali feldspar, nepheline, clinopyroxene, and some olivine. *Unit SM4* is the largest preserved unit, covering approximately 100 km^2 and has steeply outward sloping contacts. The commonest rock type is foyaite, with platy alkali feldspars and cumulate textures. The same magma composition chilled to porphyritic phonolite near structurally high-level lava xenoliths. Sub-unit HY is a body of 2 km largest dimension with variable grain size cancrinite-rich nepheline syenite that outcrops around the southern portion of the AGGD (as shown in fig. 1). The accessory phases låvenite and rinkite are found throughout SM4 but are particularly common in HY. *Unit SM5* grades rapidly from margins of lardalite (i.e. augite syenite) to a mostly cumulus-textured nepheline syenite with up to $\geqslant 30\%$ modal nepheline. The grain size may be very coarse $\sim$ 2–5 cm alkali feldspar) and very rare concentrations of euhedral red eudialyte (Zr-bearing silicate) occur. The related unit SM5* is a partial ring dyke of larvikite ('syenogabbro' of Emeleus and Harry, 1970) related to the early phase of SM5. Cryptoperthitic feldspar shows weak iridescence in hand specimen and occasional xenocrysts of plagioclase are typical. Olivine and biotite are common in SM5 and SM5*. *Unit SM6* is an irregular sill-like horizon of lujavrite (eudialyte–nepheline–microsyenite) that occurs preferentially beneath sub-horizontal lava xenoliths in unit SM4. Flow-banding is often picked out by variations in grain size and modal proportions of the essential minerals, albite, microcline, nepheline, aegirine, and eudialyte. 'Dark lujavrite', an aegirine-rich variety with phenocrysts of nepheline and eudialyte, sometimes cuts 'white lujavrite'—which has interstitial eudialyte. The lujavrites are peralkaline and comparable in bulk composition with the 'white kakortokite' from the Ilímaussaq intrusion (see Ferguson, 1970; Gerasimovsky and Kusnetsova, 1967).

Analytical procedure

All mineral analyses were performed at the University of Durham, England, with a Cambridge Instrument Company Geoscan Mk II electron microprobe, using methods similar to those of Sweatman and Long (1969). The probe was operated with an accelerating voltage of 15 kV and a beam current of 40 nA focused in general to a 3–5 μm spot. A combination of natural minerals and synthetic non-glassy compounds and elements were used for standards. Crystal spectrometer analyses (WDS) using LiF, KAP, and PET crystals were reduced by an on-line computer program equipped with ZAF correction routines written by A. Peckett, University of Durham. All iron was determined as FeO. Typical detection limits are close to 0.02 wt. %.

Mineralogy

Representative analyses of the mafic silicates are given in Tables II to VI. Their pertinent chemical substitutions are outlined below and comparisons with various studies from other plutonic centres are given for each mineral species.

Olivine is common only in the lardalitic margin of unit SM5 and in its associated partial ring dyke SM5*, and in the late AGGD. Olivine is also present in the fine-grained phonolitic margins of units SM2, SM3, and SM4. Elsewhere it is extremely rare, although it is occasionally found as corroded relics and pseudomorphs in nepheline syenites of unit SM4. Only the abundant olivines from units SM5 and SM5* have been studied in detail, but reconnaissance analyses from the earlier units indicate olivines which are even more Mn-rich for a given fayalite (Fa) content. They are plotted in terms of Fe–Mg–Mn in fig. 2 where they are compared with trends from the Ilímaussaq intrusion (Larsen, 1976), Skaergaard (Deer and Wager, 1939) and to the South Qôroq centre in the Igaliko complex (Stephenson, 1974). Based on the nomenclature for natural olivines in the system Mg_2SiO_4–Fe_2SiO_4–Mn_2SiO_4–Ca_2SiO_4 (Mossman and Pawson, 1976; Brown, 1980) the Motzfeldt olivines range from hortonolite through ferrohortonolite to iron-knebelite. They contain high MnO (1.8–5.0 wt. %) and CaO (up to 1.2 wt. %).

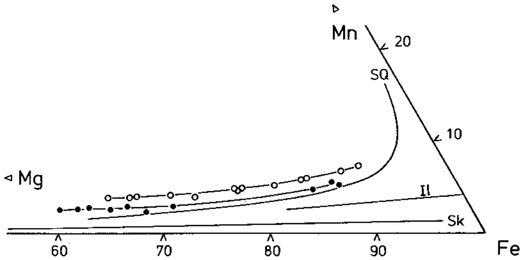

FIG. 2. Olivine; hollow circles = SM5 (lardalite); filled circles = SM5* (larvikite); SQ = South Qôroq centre (Stephenson, 1974); Il = Ilímaussaq (Larsen, 1976); Sk = Skaergaard (Deer and Wager, 1939).

Table II. Representative analyses of olivines (cores)

Unit	1. SM5*	2. SM5*	3. SM5	4. SM5	5. SM5*	6. SM5
SiO_2	33.7	33.0	31.6	31.8	31.7	31.0
TiO_2	0.13	0.08	0.11	0.10	0.12	0.11
Al_2O_3	n.d.	n.d.	0.04	0.04	n.d.	0.07
FeO^+	46.5	50.5	51.0	56.8	59.4	59.6
MnO	1.97	2.37	3.09	3.69	3.81	5.00
MgO	17.3	14.0	13.5	7.12	4.97	3.25
CaO	0.59	0.44	0.56	0.49	0.72	1.13
Na_2O	0.05	n.d.	0.03	0.10	n.d.	0.12
Total	100.24	100.39	99.93	100.14	100.72	100.28
Cations to 16 oxygens						
Si	4.008	4.010	3.906	4.046	4.070	4.043
Ti	0.012	0.008	0.010	0.010	0.012	0.010
Al	0.000	0.000	0.006	0.006	0.000	0.011
Fe	4.624	5.135	5.270	6.048	6.372	6.515
Mn	0.199	0.244	0.324	0.398	0.414	0.553
Mg	3.056	2.528	2.488	1.353	0.949	0.633
Ca	0.074	0.057	0.074	0.067	0.098	0.158
Na	0.011	0.000	0.006	0.026	0.000	0.032
Fe	58.7	64.9	65.2	77.6	82.4	84.6
Mg	38.8	32.0	30.8	17.3	12.3	8.2
Mn	2.5	3.1	4.0	5.1	5.3	7.2

n.d. = not detected. $^+$total iron. Cr and Ni below detection (0.02) in all samples.

1. 58036, larvikite.
2. AM29, larvikite.
3. AM38, lardalite
4. AM40, lardalite.
5. AM55, larvikite.
6. AM39, lardalite.

Olivines from units SM5 and SM5* form clear subparallel trends (see fig. 2) ranging from $Fa_{59}Tp_{2.5}$ to $Fa_{84}Tp_{5.2}$ in SM5 and from $Fa_{65}Tp_{3.9}$ to $Fa_{85}Tp_{7.2}$ in SM5* (Tp = tephroite, Mn_2SiO_4).

The trace elements Cr and Ni were not detected. However, small amounts of Na_2O, TiO_2, and Al_2O_3 (to 0.12, 0.13, and 0.07 wt. % respectively) from olivine cores are thought to be free from stray interferences and significant. Precise analyses of magnesian olivines from mantle-derived dunites show lesser amounts of the same oxides (Dawson *et al.* 1981; to 0.03, 0.05, and 0.06 wt. % respectively) with in addition up to 0.03 wt. % P_2O_5. Phosphorus was not analysed in the Motzfeldt olivines, although all of the olivine-bearing syenites contain apatite and it may be that the small amounts of Na represent traces of a natrophillite component ($NaMnPO_4$; Moore, 1972). Alternatively, these trace amounts could be impurities derived from unnoticed inclusions of fluids or crystals.

Clinopyroxene forms a general compositional trend from pink, grey, or colourless salites (in thin section) towards green hedenbergite and then to yellowish-green aegirine. Schiller inclusions (?rutile) are common in the magnesian salites and are characteristic of the AGGD and basic members of unit SM5. Sector zoning is present in rare quenched crystals associated with plagioclase megacrysts in the AGGD. Many of the syenites contain clinopyroxene zoned towards greener margins and often mantled by amphibole. A second generation of

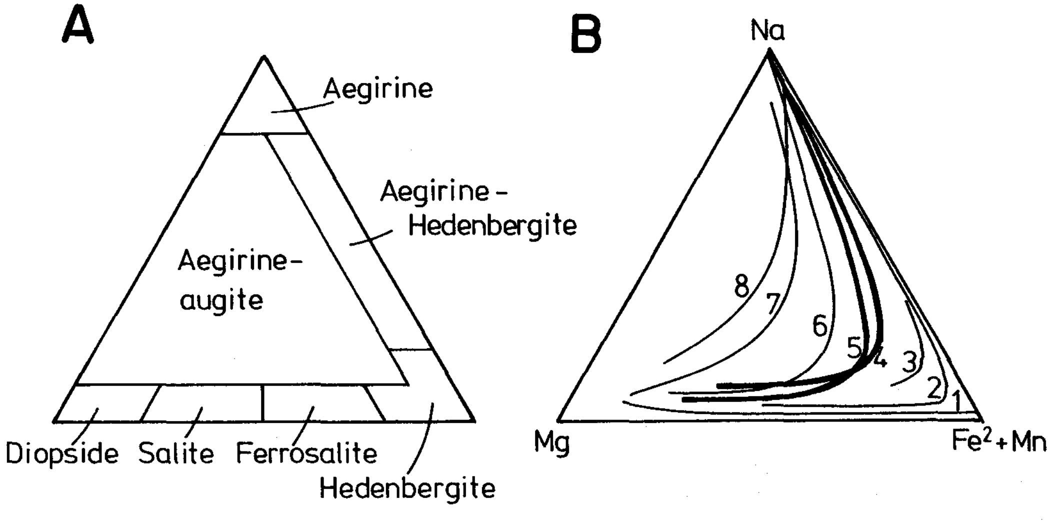

FIG. 3. Clinopyroxene. (A) Nomenclature used in this work. (B) Fractionation trends compared; 1 = Skaergaard (Brown and Vincent, 1963); 2 = Ilímaussaq (Larsen, 1976); 3 = Pantellerites (Nicholls and Carmichael, 1969); 4 and 5 = units SM4 and SM5 respectively, Motzfeldt centre (Jones, 1980; Jones and Peckett, 1980); 6 = South Qôroq centre (Stephenson, 1973); 7 = Uganda nephelinites (Tyler and King, 1967); 8 = Itipirapuã, Brazil (Gones *et al.*, 1970).

green interstitial clinopyroxene (Na-rich) is common, resulting in the sequence clinopyroxene-amphibole-clinopyroxene. Defining the clinopyroxene nomenclature as set out in fig. 3*a* (after Poldervaart and Hess, 1951; and Deer *et al.*, 1978), and attributing most Na in the Fe-poor clinopyroxenes to a jadeite ($NaAlSi_2O_6$) component, they form the trend salite, ferrosalite, aegirine-augite, aegirine-hedenbergite, aegirine. The two most complete trends from Motzfeldt (units SM4 and SM5) are compared with those from other igneous environments in fig. 3*b*, in terms of Mg-(Fe^{2+} + Mn)-Na. The Motzfeldt clinopyroxenes clearly fall between trends for the South Qôroq centre and the Ilímaussaq intrusion (curves 6 and 2 in fig. 3*b*), and show a superficial resemblance to the pantellerite trend (curve 3 in fig. 3*b*), whose clinopyroxenes differ, when all of the elements are considered. The Motzfeldt trends are especially similar to a trend for the Hviddal dyke illustrated by Stephenson and Upton (1982; their fig. 3).

The substitutions can be considered with reference to the general formula $X^{viii}Y^{vi}Z_2^{iv}O_6$, and variations in the cation proportions of analysed elements are shown in fig. 4, relative to the index Na-Mg. Ferric iron was calculated for the plotted positions in fig. 4. Calculations of Fe^3/Fe^2 from electron probe analyses are often notoriously imprecise (e.g. Finger, 1972). However, the procedure followed that outlined in Jones and Peckett (1980) and is comparable with that used by other workers in the Gardar province. Thus the dashed lines for Fe^2 and Mn in fig. 4 indicate the trends for clinopyroxene from the Ilímaussaq intrusion (Larsen, 1976); note the higher Mn-content of the Motzfeldt clinopyroxenes. The *Z* position is essentially occupied by Si and Al, the ratio Si/(Si + Al) increasing with rising Na-Mg, even when analytical error in Si (approximately ±0.5 at 50.0 wt. % SiO_2) is taken into account. The sum (Ca + Na) which dominates the *X* position may be as low as 0.90 in the salites, although it is usually between 0.92 and 0.96, rising through the ferrosalites to 0.98.

Table III. Selected analyses of clinopyroxenes from units SM4 (1-6) and SM5 (7-12).

Sample	1. AM45a	2. AM68	3. AM51	4. AM48	5. 63746	6. 63729	7. AM39b	8. AM38	9. AM88	10. AM110	11. AM77	12. AM110
SiO_2	50.3	51.7	51.3	49.0	51.0	52.2	52.1	50.3	50.5	49.9	51.0	52.8
TiO_2	0.32	0.41	0.30	0.33	0.37	0.60	1.06	0.77	0.31	0.54	0.73	1.13
ZrO_2	0.12	0.07	0.37	0.53	0.67	1.53	n.d.	n.d.	0.07	0.45	1.45	0.02
Al_2O_3	2.45	0.98	0.96	0.67	0.77	0.82	2.09	2.00	1.11	0.87	0.68	3.16
$FeO^†$	13.0	15.7	22.0	25.2	26.9	26.8	11.1	12.4	16.7	22.0	25.2	26.2
MnO	0.77	0.84	1.37	1.11	0.76	0.44	0.64	0.67	1.38	1.21	0.83	0.16
MgO	9.09	8.13	3.04	0.91	0.42	0.20	11.4	10.3	6.97	3.37	1.33	0.21
CaO	21.6	20.7	14.2	14.7	7.03	2.33	21.1	23.4	20.3	18.5	7.93	0.05
Na_2O	1.50	1.30	4.68	5.32	10.1	12.5	0.92	0.71	1.21	3.74	8.87	13.5
K_2O	0.01	0.01	n.d.	0.01	0.01	n.d.	n.a.	n.d.	n.d.	0.03	0.01	0.02
Total	99.16	99.84	98.22	97.78	98.03	97.42	100.41	100.55	98.55	100.61	98.03	97.25
Cations to 6 oxygens												
Si	1.944	1.999	2.066	2.035	2.101	2.145	1.954	1.917	1.994	1.989	2.087	2.135
Ti	0.009	0.012	0.009	0.010	0.011	0.019	0.030	0.022	0.009	0.016	0.023	0.034
Zr	0.002	0.001	0.007	0.011	0.011	0.031	0.000	0.000	0.001	0.009	0.029	0.000
Al	0.112	0.045	0.046	0.033	0.037	0.040	0.093	0.090	0.052	0.041	0.033	0.150
$Fe^†$	0.422	0.508	0.742	0.875	0.928	0.922	0.348	0.396	0.552	0.734	0.863	0.886
Mn	0.025	0.028	0.047	0.039	0.026	0.015	0.020	0.022	0.046	0.041	0.029	0.006
Mg	0.524	0.468	0.183	0.057	0.026	0.012	0.636	0.585	0.411	0.200	0.081	0.013
Ca	0.896	0.856	0.612	0.654	0.310	0.103	0.847	0.957	0.858	0.792	0.348	0.002
Na	0.112	0.097	0.366	0.429	0.805	0.996	0.067	0.053	0.093	0.289	0.704	1.058
K	0.001	0.001	0.000	0.001	0.000	0.000	0.000	0.000	0.000	0.001	0.001	0.001
Na	11.4	9.6	36.3	42.3	74.4	95.0	6.7	5.3	9.1	30.0	67.5	98.3
Fe^2+Mn	35.2	44.2	45.6	52.1	23.3	3.8	30.4	38.0	50.6	49.2	24.7	0.5
Mg	53.4	46.2	18.1	5.6	2.3	1.2	62.9	56.7	40.3	20.8	7.8	1.2
Zr/px[a]	0.2	0.1	0.7	1.0	1.3	3.0	0.0	0.0	0.1	0.8	2.8	0.0

[†] total iron as FeO causes low totals and high Si in recalculations; to first approximation Fe^3 = Na (from cation proportions). [a] Zr end-member components calculated after Jones and Peckett (1980).

n.d. = not detected, n.a. = not analysed.

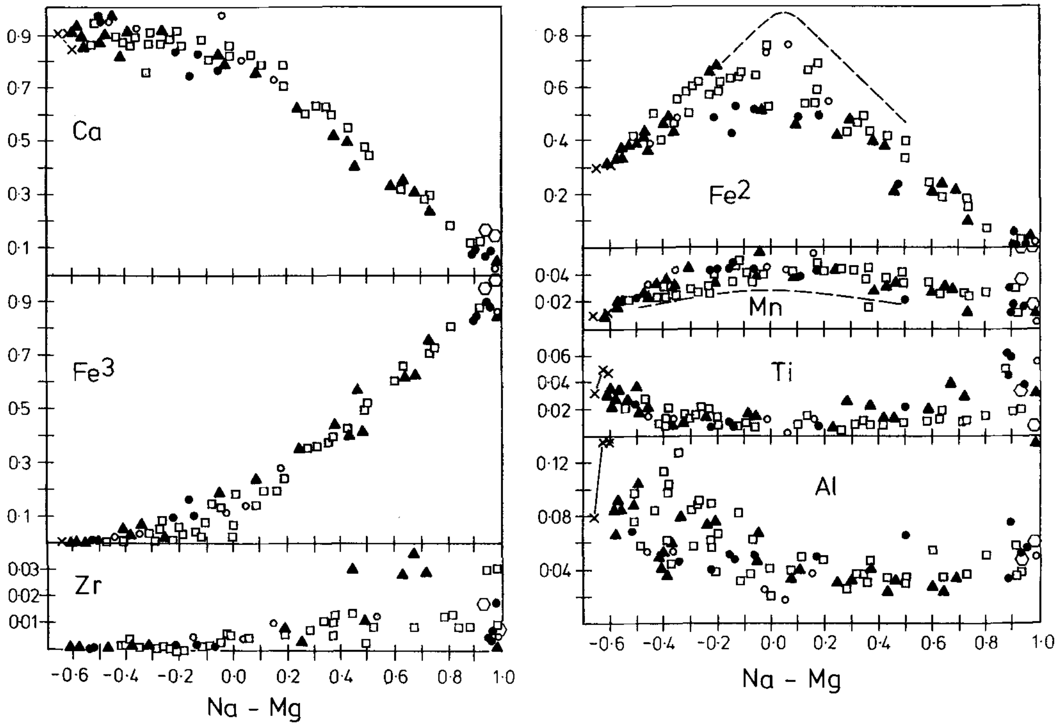

FIG. 4. Clinopyroxene chemical variation; cation proportions to 6 oxygens with Fe^{3+} calculated according to procedure outlined in Jones and Peckett (1980) or, in a few cases, estimated from $Fe^3 = Fe_{total} - Na$; filled circles = SM1; open circles = SM2/3; open squares = SM4; filled triangles = SM5 (and SM5*); open hexagons = SM6; crosses = AGGD; dashes = part of trend for Ilímaussaq (after Larsen, 1976); some data omitted for clarity.

This is probably a direct result of Ca-poor pyroxene in solid solution in the early clinopyroxenes (Larsen, 1976). With increasing Na, (Na+Ca) approximates to unity, as is normal for alkali clinopyroxene. Minor K is often present (to 0.05 wt. % K_2O) in the more sodic samples, possibly reflecting minor amounts of K-acmite. In addition to Fe, Mg, and Mn, the *Y* position involves substitution of higher valence elements such as Al, Ti, and Zr. Divalent Mg, Fe, and Mn are progressively replaced by trivalent iron in balance to Na in *X*, to form the acmite component ($NaFe^3Si_2O_6$). Occasional aegirines contain high Al, with up to 11 mole % jadeite in one zoned example from unit SM5.

Ti is apparently present as $NaTiSiAlO_6$ in the early clinopyroxene, with both Al and Ti falling with increasing Na-Mg, followed by a resumption of high but variable levels in the Na-rich samples (see fig. 4). Insufficient Na in the salites to account for all of the Al as jadeite, suggests some calcium-Tschermaks component, $CaAlSiAlO_6$ (CaTs), with up to 3 and 5 mole % CaTs in SM5 and the AGGD respectively. A rare example of sector zoning in lilac-coloured salite from the AGGD corresponds to large differences in Al and Ti between sectors. This is illustrated in fig. 4 (crosses linked by a line) and is reminiscent of similarly sector zoned pyroxenes described by Downes (1974) and Hollister and Gancarz (1971).

Zr is an important constituent of the Motzfeldt clinopyroxenes, increasing with Na and Fe (fractionation), sometimes reaching 1 or 2 and rarely up to 7.0 wt. % ZrO_2, with Zr/Hf ratio remaining at about 35. A more detailed discussion has been presented by Jones and Peckett (1980), where the status of the required end member, $Na(Fe^2,Mg)_{0.5}Zr_{0.5}Si_2O_6$ was evaluated. The most Zr-rich varieties may have been derived from trapped liquids and are only found in the absence of other Zr-bearing phases such as eudialyte or zircon. Anomalously low Zr in relatively fractionated clinopyroxene throughout some syenite samples may signal co-precipitation of eudialyte and a similar argument was given for different units at Ilímaussaq, where eudialyte is far more abundant

(Larsen, 1976). It is worth emphasizing that in general the clinopyroxene trends are composite, in as much as there is frequently an overgrowth of amphibole separating zoned clinopyroxene cores and rims from interstitial Na-rich clinopyroxene. A similar sequence involving stable amphibole between core, rim, and interstitial clinopyroxene to that established for Ilímaussaq (Larsen, 1976) could be used for Motzfeldt. This scheme would be less precise for the Motzfeldt pyroxenes since specific clinopyroxene compositions do not always define the onset of amphibole crystallization throughout any one of the syenite units.

Amphibole is the commonest mafic mineral and has characteristically anhedral outlines. The amphibole adopts a wide range of colours, reflecting changing composition with increasing fractionation of the host magma. In general terms, brown pleochroic amphibole in the basic syenites, such as the larvikites of SM5*, gives way to abundant greenish amphibole, typical of most of the nepheline syenites, and are succeeded by less common blue-green or green-blue amphibole in the most fractionated syenites and in the lujavrites. In addition, there is often outward zonation of the individual amphiboles through part of the same sequence of colours, corresponding to alkali(Na)-enriched rims.

The amphiboles are all iron-rich varying from hastingsite through ferroedenite to arfvedsonite, using either the Leake (1978) or Phillips (1966) terminology, with arfvedsonite being represented by ferroeckermannite in the latter. To avoid detailed terminology, which is often cumbersome, the data are simply presented as a series of x–y plots (fig. 5) using Na^x-Al^z as an index (after Larsen, 1976) where the superscripts ^{x,z} refer to site occupancy in the general formula $AX_2Y_5Z_8O_{22}(OH,F)_2$. Most of the analyses were run through a computer program MINDATA5 (J. L. Knight, University of Durham) which estimated Fe^3/Fe^2 following the Phillips (1966) scheme. The procedure is similar to that advocated by Leake (1978) where Fe^3/Fe^2 is increased until stoichiometry is achieved for recalculation of the anhydrous analysis to 23 oxygens. This yields slightly different values of Na^x-Al^z than does retention of total iron as FeO, though it has a negligible effect on the overall trends.

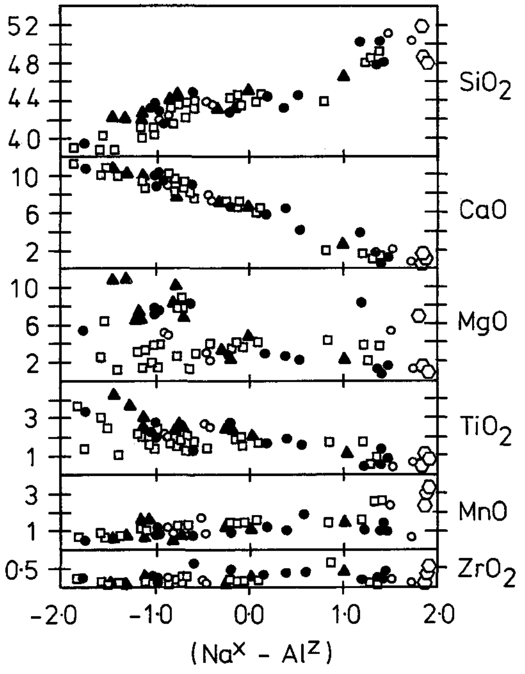

FIG. 5. Amphibole compositional variation; symbols as in fig. 4; (Na^x-Al^z) derived from anhydrous analyses recalculated to 23 oxygens and from program MINDATA5 (see text for details); some data omitted for clarity.

Increasing SiO$_2$ and decreasing CaO with rising Na^x-Al^z is a consistent trend for the Motzfeldt amphiboles (fig. 5), conforming to the substitution Ca^x + Al^z = Na^x + Si^z. This is identical to that found in the adjacent North Qôroq centre (Chambers, 1976), in the other Igaliko centres (Stephenson, 1973; Powell, 1978) and in other centres throughout the Gardar province (e.g. Anderson, 1974; Larsen, 1976). There is a systematic fall in Ti, agreeing with the observations of Helz (1973) for amphiboles in general, where proceeding fractionation was accompanied by lowering temperatures and, or, increasing oxygen fugacity (f_{O_2}). Cawthorn (1976) maintains that TiO$_2$ is proportional to total pressure, although stabilization down-temperature of other Ti-minerals, such as Fe–Ti oxides, sphene, and rinkite may be far more important. Mn increases with Na^x-Al^z (0.5–3.3 wt. % MnO) and is usually highest at the margins of zoned crystals, and in the lujavrites (unit SM6). The Mn levels are consistently higher than for otherwise comparable amphiboles from the Ilímaussaq intrusion (Larsen, 1976; total range 0.4–1.0 wt. %), but are similar to amphiboles from the North Qôroq centre (Chambers, 1976) of the Igaliko complex. Zr is usually present in small amounts (0.1–0.8 wt. % ZrO$_2$) but varies unpredictably, generally being less than in adjacent clinopyroxene. Larsen (1976) found that Zr in amphibole from Ilímaussaq is approximately one-half the amount found in coexisting clinopyroxene. Zr is below detection limits (~ 0.02 wt. % ZrO$_2$) in amphibole from the lujavrites (SM6) where its interstitial habit suggests that it crystallized after

Table IV. Representative analyses of amphiboles.

Unit Colour†	1. SM1 Bw	2. SM4 Bw/Gn	3. SM5* Bw	4. SM4 Bw	5. SM1 Bw/Gn	6. SM5 Bw/Gn	7. SM4 Gn/Bw	8. SM1 Bl	9. SM6 Bl/Gn	10. SM6 Bl/Gn
SiO_2	39.8	40.2	42.8	43.2	42.9	44.1	48.2	48.0	47.2	52.9
TiO_2	3.46	2.66	2.95	2.50	3.06	2.45	1.87	0.63	0.85	0.66
ZrO_2	0.28	0.05	0.27	0.14	0.40	n.a.	0.09	0.18	0.50	0.02
Al_2O_3	10.5	9.50	10.9	6.76	5.93	5.88	3.20	2.36	3.13	1.17
FeO*	22.9	22.3	19.0	20.1	28.0	27.8	29.0	33.2	31.1	19.3
MnO	0.63	0.82	0.47	0.92	1.31	1.35	1.65	1.22	3.05	2.64
MgO	5.51	6.32	6.66	8.12	3.02	3.48	3.20	0.72	0.56	7.11
CaO	11.3	10.8	9.78	10.1	7.41	7.44	1.62	1.72	1.41	0.23
Na_2O	2.74	3.55	3.77	3.69	5.23	5.03	8.17	7.24	8.38	9.97
K_2O	1.63	1.19	1.50	1.54	1.61	1.37	1.57	1.46	1.53	2.27
Total	98.75	97.39	98.10	97.07	98.87	98.90	98.57	96.73	97.71	96.27
Cations to 23 oxygens										
Si	6.218	6.345	6.522	6.739	6.832	6.962	7.587	7.834	7.884	7.734
Ti	0.406	0.316	0.338	0.294	0.367	0.291	0.222	0.077	0.105	0.073
Zr	0.021	0.004	0.020	0.011	0.031	0.000	0.007	0.014	0.040	0.002
Al	1.929	1.768	1.966	1.245	1.115	1.096	0.595	0.454	0.603	0.201
Fe	2.985	2.942	2.418	2.626	3.737	3.680	3.824	4.527	4.250	2.361
Mn	0.083	0.110	0.061	0.122	0.177	0.181	0.220	0.169	0.422	0.313
Mg	1.282	1.487	1.513	1.890	0.717	0.820	0.752	0.176	0.137	1.498
Ca	1.887	1.818	1.596	1.697	1.266	1.260	0.274	0.301	0.247	0.038
Na	0.829	1.086	1.115	1.117	1.617	1.542	2.500	2.290	2.651	2.708
K	0.326	0.240	0.291	0.307	0.327	0.276	0.316	0.303	0.319	0.406
Na^x-Al^z	-1.67	-1.47	-1.07	-0.96	-0.43	0.14	1.31	1.53	1.64	1.70
(± n)	(-1.72)	(-1.52)	(-1.10)	(-0.93)	(-0.23)	(-0.34)	(1.20)	(1.35)	(1.84)	(1.80)

†dominant colours from pleochroic scheme, Bw = brown, Gn = green, Bl = blue. *total Fe. (n) = Na^x-Al^z obtained from computer programme MINDATA5 (Knight, Durham University) estimating Fe^3 and used in plotting figure 5.

1 = 63703, syenite. 2 = 58039, olivine-bearing ne-syenite. 3 = AM55, larvikite. 4 = 58066, core of large grain from intercumulus band in ne-syenite. 5 = 54132, ne-syenite. 6 = AM85, ne-syenite. 7 = 58066, rim analysis to 4. 8 = 63760, ne-syenite. 9 = AM159, white lujavrite. 10 = AM140, dark lujavrite.

Table V. Representative analyses of micas.

Unit	1. SM5*	2. SM5*	3. SM3	4. SM4
SiO_2	36.3	35.8	36.3	35.6
TiO_2	6.80	7.38	4.42	3.21
Al_2O_3	13.2	12.2	10.7	10.4
FeO†	17.4	22.3	32.5	31.2
MnO	0.18	0.60	0.96	2.15
MgO	12.5	8.15	4.00	2.81
CaO	0.10	0.09	0.12	0.03
Na_2O	0.51	0.32	0.29	0.16
K_2O	8.92	8.96	8.12	8.91
Total	95.91	95.80	97.41	94.47
Cations to 22 oxygens				
Si	5.469	5.576	5.800	5.909
Ti	0.771	0.864	0.531	0.401
Al	2.360	2.246	2.013	2.045
Fe	2.195	2.907	4.344	4.339
Mn	0.022	0.081	0.130	0.303
Mg	2.816	1.819	0.953	0.695
Ca	0.016	0.015	0.020	0.006
Na	0.148	0.098	0.090	0.050
K	1.714	1.780	1.656	1.888
Fe/Fe+Mg	0.44	0.61	0.82	0.86
Al^z	2.53	2.42	2.20	2.09
Al/Al+Si	0.31	0.29	0.26	0.26

†total iron. $Al^z = (Al+Ti)^z$

1 = 58037, (larvikite) large plates.

2 = 58062, (larvikite) rim to Ti-magnetite.

3 = 58400, (syenite) interstitial grain.

4 = 63746, (ne-syenite) interstitial grain.

eudialyte. K shows little variation and remains remarkably constant throughout all of the syenites (total variation 1.2–2.3 wt. % K_2O). This may reflect buffering from a liquid which was itself subject to K-rich feldspar fractionation. The ratio Na/K in the amphiboles ranges from about 2.4 in the larvikitic syenites (SM5*) to about 7.0 in the lujavrites; almost identical to the range exhibited by amphiboles from the Ilímaussaq intrusion (Larsen, 1976).

Mica is uncommon in most of the nepheline syenites and correspondingly few analyses have been made. Biotite forms anhedral orange-brown plates up to 2 cm across and radiating overgrowths on Fe–Ti oxides in the mafic syenites of SM5 and SM5*. Paler coloured, brown or green biotite occurs sporadically as a minor phase in the syenites and may form up to 3% of the mode in parts of unit SM4.

Referring to a general formula for biotite, $X_2Y_{4-6}Z_8O_{22}(OH,F)_4$, there is evident variation in the Al content of the tetrahedral site (Al^z, which includes Ti^z) corresponding to increasing Si^z/Al^z with increasing degree of fractionation of the host rock, in the order alkali-gabbro, larvikite, syenite, nepheline-syenite. Similarly the ratio Fe/(Fe+Mg) increases and is compared with other trends in

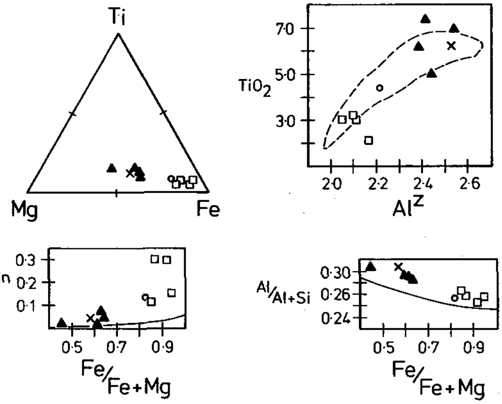

FIG. 6. Micas; symbols as in fig. 4; dashed field = locus of data from North Qôroq centre (from Chambers, 1976); solid curve in Fe/(Fe+Mg) plots = trend for Klokken micas (after Parsons, 1979).

fig. 6. Sodium (Na^x) shows a steady decrease with decreasing Al^z (not illustrated) and TiO_2 drops markedly from 7.3 to 2.1 wt. % over the range of fractionation examined, and is comparable with more abundant micas from the North Qôroq centre (locus outlined with dashes in fig. 6). MnO increases from 0.2 to a maximum of 2.7 wt. %, which is approximately 7 mole % manganophyllite component (Mang) compared with $Mang_{1.0}$ from the Klokken intrusion (Parsons, 1979) and $Mang_{45}$ from the soda syenites from Shonkin Sag laccolith (Nash and Wilkinson, 1970). CaO is present at normally low levels (up to 0.15 wt. %) and Zr was below detection in all samples.

Aenigmatite is important only in the fine-grained phonolites of units SM2 and SM3, where it forms dark-brown poikilitic plates which enclose small feldspars, nephelines, and corroded Fe–Ti oxide relics. It is sporadically present in the most fractionated parts of units SM4 and SM5. The average analyses of four grains (Table VI) indicate a coupled substitution of the type $Ca^xAl^z = Na^xSi^z$, referring to the general formula $X_2Y_6Z_6O_{20}$. This is clearly seen in fig. 7, and the same substitution predominates in zoned aenigmatites from Ilímaussaq (Larsen, 1977), the fields for which are outlined in fig. 7. With the small number of analyses available it is not possible to substantiate a bimodal distribution, like the core and rim populations from Ilímaussaq, and the analysed grains were apparently homogeneous. Mg is higher than recorded at Ilímaussaq (up to 0.82 versus 0.03 wt. % MgO) while ZrO_2 is at a similarly low level to Ilímaussaq (0.1–0.2 wt. %). Mn is more extensively enriched with fractionation (Na) at Motzfeldt (1.8 to 2.7 wt. % MnO) than found in otherwise comparable examples from Ilímaussaq (0.7–0.9 wt. %).

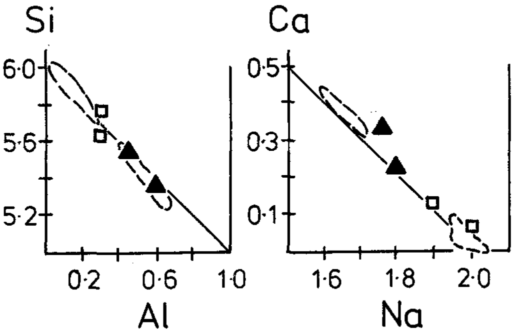

FIG. 7. Aenigmatites; symbols as in fig. 4; dashed field = loci of data for zoned aenigmatites from Ilímaussaq (Larsen, 1977).

Table VI. Representative aenigmatite analyses.

Unit	1. SM4	2. SM4	3. SM5	4. SM5	
SiO_2	38.2	39.1	38.3	36.5	
TiO_2	8.50	7.00	8.37	8.49	
Al_2O_3	1.59	1.63	2.56	3.26	
FeO*	40.5	40.1	40.2	40.5	
MnO	2.72	2.35	1.93	1.75	
MgO	0.46	0.39	0.82	0.49	
CaO	0.49	0.85	1.42	2.29	
Na_2O	7.07	6.61	6.35	6.20	
K_2O	0.02	0.03	0.02	0.04	
Total	99.55	98.06	99.97	99.52	
Cations to 20 oxygens					
Si	5.523	5.721	5.556	5.289	6.00
Al	0.270	0.283	0.437	0.558	
Fe^3	0.207	0.000	0.007	0.153	
Fe^2	4.697	4.916	4.872	4.758	6.00
Ti	0.923	0.771	0.938	0.925	
Mn	0.334	0.292	0.178	0.215	
Ca	0.046	0.021	0.012	0.102	
Ca	0.030	0.112	0.209	0.254	6.00
Na	1.969	1.878	1.784	1.740	
K	0.004	0.006	0.003	0.008	

*total iron; Fe^3 calculated assuming stoichiometry. 1= AM7, interstitial small grains. 2 = 58066, core of large anhedral grain. 3 = AM82, core of large anhedral grain from eudialyte-bearing sample. 4 = AM43, core of large (5mm) anhedral grain.
All samples are ne-syenites, and analyses are the averages of two or more analyses.

Discussion

In its intrusive styles and mineralogical trends the Motzfeldt centre shows similarities to the other three centres of the Igaliko complex. In detail, several features of the mafic silicates more closely overlap those of the North Qôroq centre (Chambers, 1976), and both the North Qôroq and Motzfeldt centres are more fractionated in general, than the younger South Qôroq (Stephenson, 1972, 1973, 1974, 1976) and Igdlerfigssalik (Powell, 1976, 1978) centres. The last major units in the Motzfeldt centre (SM5, AGGD) contain the most basic rocks, although unit SM5 fractionated *in situ* from larvikitic margins to eudialyte-bearing nepheline syenite in its interior. Successive intrusions of silica undersaturated magmas and their *in situ* fractionation lead to extensive and often repeatedly overlapping variations in the mafic silicates. The end products of such efficient fractionation are expressed by the presence of lujavrites (SM6) and it is these rocks which bear the most extreme mineral compositions.

Olivine was absent from the liquidus in all but the most basic syenites, perhaps because of rather high f_{O_2}, and low silica activity, causing a reaction of the type

$$\underset{\text{fayalite}}{3Fe_2SiO_4} + O_2 \rightarrow \underset{\text{magnetite}}{2Fe_3O_4} + 3SiO_2$$

As pointed out by Larsen (1976) the fayalite-magnetite-quartz (FMQ) buffer given above, may represent lower f_{O_2} conditions for more silica undersaturated magmas. The rare occurrences of relic olivines in some of the syenites suggest that olivine may have been an early formed phase and much more abundant at Motzfeldt, but subsequently replaced by other minerals. This is certainly suggested for Ilímaussaq, where Larsen (1976) discovered relic olivines even in quite fractionated rocks. Elsewhere in the Igaliko complex corroded olivine relics were apparently partially replaced by amphibole (e.g. units SI5 and SI6 of the Igdlerfigssalik centre; Emeleus and Harry, 1970) although no such specific process was recognized at Motzfeldt. Low f_{O_2} conditions probably prevailed in the early stages of each Motzfeldt magma, where Fe-rich olivine and Ti-magnetite (Jones, 1980) were stable. That f_{O_2} increased with fractionation is evident from the consistent clinopyroxene trends towards acmite, which is rich in ferric iron. However, substitution of Zr in aegirines (Zr/px) may require Fe^{3+}/Fe^{2+} charge balance (Jones and Peckett, 1980) and because Zr/px varies considerably, even on the scale of a thin section, complex changes in f_{O_2} probably occurred in some of the residual trapped liquids.

The occurrence of aenigmatite in the more fractionated syenites and as overgrowths to magnetite grains in marginal phonolites of units SM2, SM3, and SM4 is consistent with a peralkaline condition (e.g. Hodges and Barker, 1973) which Nicholls and Carmichael (1969) relate to the activity of sodium disilicate ($Na_2Si_2O_5$) in the liquid. The local development of peralkalinity in late-crystallizing trapped liquid agrees with the occasional very high Zr contents of some interstitial aegirine (Jones and Peckett, 1980) and is in accord with the experimental results of Watson (1979) who demonstrated high solubility of Zr in peralkaline felsic melts.

Mn increases with fractionation in all of the mafic silicates. The resumption of lower Mn levels in the most fractionated clinopyroxenes may reflect their relatively late crystallization, postdating such Mn-rich phases as amphibole, or may merely correlate closely with Fe^{2+}. In general the mafic silicates from the Motzfeldt and South Qôroq centres (Stephenson, 1972, 1974) have similar Mn levels, both being significantly higher (2-3 times) than corresponding mafic silicates from the Ilímaussaq intrusion (Larsen, 1976, 1977). This is curious since the latter two centres have similar average Mn contents of approximately 0.25 wt. % MnO (Gerasimovsky and Kusnetsova, 1967; Stephenson, 1973) and average MnO contents for the Motzfeldt units are in the same range (0.24, 0.21, 0.23, 0.19, 0.22, 0.28 wt. %, SM1 to SM6 respectively; Jones, 1980). Larsen attributes this apparent dilemma to exclusion of Mn from available lattice sites at Ilímaussaq by vigorously high Fe^{2+} activities. A similar argument could be made for the Motzfeldt magmas, and it is significant that the separate Mn phase, Mn-pectolite (15.5 wt. % MnO; Jones, 1980) occurs both in the Motzfeldt centre of the Igaliko complex and also at Ilímaussaq (Larsen, 1976), always in the latest stages of crystallization. However, it is probably incorrect to assume that the compositions of bulk syenites necessarily represent liquids, especially where cumulate textures are present, such as in the North Qôroq and Motzfeldt centres. Since Mn appears to partition preferentially into Fe-rich olivine (e.g. Stephenson, 1974), felsic or mafic (olivine-bearing) cumulates formed from the same magma may be Mn-depleted or enriched respectively. Thus one explanation would be that in order for the comparatively felsic cumulates of the Motzfeldt centre to have similar average Mn contents to the more mafic South Qôroq centre, the parental Motzfeldt magmas had to be more Mn-rich. In the simplest sense, the Motzfeldt syenites might represent olivine-depleted, and thus Mn-depleted cumulates, with olivine-bearing syenites more similar to South Qôroq, but even richer in Mn, existing below current exposure levels. Crystallization of the opaque oxides undoubtedly played an important role in the evolution of the Motzfeldt syenites. These will be major repositories of Fe and Ti, and can carry appreciable amounts of Mg and Mn, all of which are important in the mafic silicates. Fe-Ti oxides are present as early formed phases in the basic syenites but rapidly fade out and are minor or absent throughout most of the Motzfeldt syenites; they are sometimes clearly replaced by aenigmatite (see Table I). Perhaps a comparative paucity of opaque oxide crystallization in the Motzfeldt syenites contributed to the build up of Mn, as expressed in the mafic silicates.

The development of lujavrites and of similar rock types in the peralkaline Ilímaussaq intrusion (Larsen, 1976) and at Motzfeldt, both of which were formed by multiple injections of magma, is an indication that such multiple processes are essential to their petrogeneses. Analogies and comparisons have been made throughout this paper between the mineralogies of the Motzfeldt centre and the peralkaline Ilímaussaq intrusion. The Motzfeldt centre thus provides a link between the bulk of silica undersaturated syenite plutons in the Gardar province and the separate peralkaline magmas at Ilímaussaq. The simplest model might predict that nepheline syenite batholiths, similar in all respects to the Motzfeldt centre, could have been the precursors to the formation of the Ilímaussaq intrusion.

Lastly, it should be pointed out that many of the features of the mafic silicates from the silica undersaturated syenites at Motzfeldt are similar not only to Ilímaussaq but also to silica-saturated and oversaturated complexes, such as the Kûngnât Fjeld complex recently described by Stephenson and Upton (1982). Here, they attempted to relate certain differences in amphibole trends to the degree of silica saturation of the igneous suites and noted the more prominent effects caused by the development of peralkalinity in the host magmas. Overall, it appears that the mineralogical similarities among the mafic silicates reflect the alkaline nature of the Proterozoic Gardar magmas, much more than they reflect the degree of silica saturation, and as such may be worthy of renewed experimental investigation.

Acknowledgements. This work was conducted as part of a Ph.D. thesis at the University of Durham, during tenure of a NERC grant under the supervision of Dr C. H. Emeleus, to whom I am grateful, and to Professors G. M. Brown and M. H. P. Bott for making available the facilities of the Department. Dr A. Peckett gave invaluable assistance with the electron probe and R. Phillips helped with the amphiboles. The Greenland Geological Survey (GGU) kindly provided field support and this paper is published with the permission of the Director of GGU. Sample numbers belonging to GGU are signified throughout the text by five figure numbers. The manuscript has benefited considerably from reviews by C. H. Emeleus, L. M. Larsen, and two anonymous reviewers.

REFERENCES

Anderson, J. G. (1974) *The geology of Alangorssuaq, Northern Nunarssuit complex, S. Greenland.* Ph.D. thesis, Univ. of Aberdeen (unpubl.).

Blaxland, A. B., van Breeman, O., Emeleus, C. H., and Anderson, J. G. (1978) *Bull. Geol. Soc. Am.* **89**, 231–44.

Brown, G. E. (1980) In *Reviews in Mineralogy 5; Orthosilicates* (P. H. Ribbe, ed.), Mineral. Soc. Am., Washington.

Brown, G. M., and Vincent, E. A. (1963) *J. Petrol.* **4**, 175–97.

Cawthorn, R. G. (1976) *Geochim. Cosmochim. Acta* **40**, 1319–28.

Chambers, A. D. (1976) *The petrology and geochemistry of the North Qôroq Centre, Igaliko Complex, South Greenland.* Ph.D. thesis, Univ. of Durham (unpubl.).

Dawson, J. B., Hervig, R. L., and Smith, J. V. (1981) *Fortschr. Mineral.* **59**, 303–24.

Deer, W. A., and Wager, L. R. (1939) *Am. Mineral.* **24**, 18–25.

——Howie, R. A., and Zussman, J. (1978) *Rock-Forming Minerals. Vol. 2A: Single Chain Silicates.* Longmans, London.

Downes, M. J. (1974) *Contrib. Mineral. Petrol.* **47**, 187–96.

Emeleus, C. H., and Harry, W. T. (1970) *Meddels. Grønland,* **186**, No. 3; also *Bull. Grønlands Geol. Unders.* No. 85.

——and Upton, B. G. J. (1976) In *Geology of Greenland* (A. Escher and W. S. Watt, eds.). Geol. Survey Greenland, Copenhagen, 152–81.

Ferguson, J. (1970) *Can. Mineral.* **10**, 335–49.

Finger, L. W. (1972) *Carnegie Inst. Wash. Yearb.* **71**, 600–3.

Gerasimovsky, V. J., and Kusnetsova, S. Ya (1967) *Geochem. Int.* **4**, 236–46.

Gomes, C. de B., Moro, S. L., and Dutra, C. V. (1970) *Am. Mineral.* **55**, 224–30.

Helz, R. T. (1973) *J. Petrol.* **14**, 249–302.

Hodges, F. N., and Barker, D. S. (1973) *Carnegie Inst. Wash. Yearb.* **72**, 578–81.

Hollister, L. S., and Gancarz, A. J. (1971) *Am. Mineral.* **56**, 959–79.

Jones, A. P. (1980) *The petrology and structure of the Motzfeldt Centre, Igaliko, South Greenland.* Ph.D. thesis, Univ. of Durham (unpubl.).

——and Peckett, A. (1980) *Contrib. Mineral. Petrol.* **75**, 251–5.

Larsen, L. M. (1976) *J. Petrol.* **17**, 258–90.

——(1977) *Lithos,* **10**, 257–70.

Leake, B. E. (1978) *Mineral. Mag.* **42**, 533–63.

Moore, P. B. (1972) *Am. Mineral.* **57**, 1333–44.

Mossman, D. J., and Pawson, D. J. (1976) *Can. Mineral.* **14**, 479–86.

Nash, W. P., and Wilkinson, J. F. G. (1970) *Contrib. Mineral. Petrol.* **25**, 241–69.

Nicholls, J., and Carmichael, I. S. E. (1969) Ibid. **20**, 268–94.

Parsons, I. (1979) *J. Petrol.* **20**, 653–94.

Phillips, R. (1966) *Mineral. Mag.* **33**, 1097–109.

Pitcher, W. S., and Bussell, M. A. (1977) *J. Geol. Soc. Lond.* **133**, 249–56.

Poldervaart, A., and Hess, H. H. (1951) *J. Geol.* **59**, 472–89.

Powell, M. (1976) *Theoretical, geochemical and petrological study of the Igdlerfigssalik nepheline syenite intrusion, Greenland.* Ph.D. thesis, Univ. of Leeds (unpubl.).

——(1978) *Lithos,* **11**, 99–120.

Stephenson, D. (1972) Ibid. **5**, 187–201.

——(1973) *The petrology and mineralogy of the South Qoroq Centre, Igaliko Complex, South Greenland.* Ph.D. thesis, Univ. of Durham (unpubl.).

——(1974) *Lithos,* **7**, 35–41.

——(1976) *Bull. Grønlands Geol. Unders.* No. 118.

——and Upton, B. G. J. (1982) *Mineral. Mag.* **46**, 283–300.

Sweatman, T. R., and Long, J. V. P. (1969) *J. Petrol.* **10,** 332–79.

Tyler, R. C., and King, B. C. (1967) *Mineral. Mag.* **36,** 5–22.

Upton, B. G. J. (1974) In *The Alkaline Rocks* (H. Sørenson, ed.). J. Wiley and Sons, London. 221–38.

Watson, E. B. (1979) *Contrib. Mineral. Petrol.* **70,** 407–19.

[*Manuscript received 4 May 1983;*
revised 10 June 1983]